7
UWB Antenna for WBAN Application

The design of a wireless communication system, which works in the proximity of human body, requires an investigation of antenna-human body interaction. One of the utmost promising applications of UWB technology is in WBAN, due to its key features such as high data transmission capacity at low power level. In order to acquire the healthcare data of patient in the proximity of human body, BAN can be classified in the three categories: in-body, on-body and off-body. These applications continuously update the real time patient's status to the health care professionals, which helps them to provide preventive, curative and rehabilitative health care services in a systematic way. In this chapter, we have investigated the performance of fractal UWB antenna and fractal UWB MIMO antenna for on/off-body communications. It is evident that antenna characteristics are influenced because of water and body tissues of human body. Thus, the measurement in the proximity of human body and layered human tissue model is performed in terms of S-parameters and radiation patterns. These results demonstrate that fractal antennas are an appropriate choice for BAN applications.

7.1 Introduction

The UWB technology provide a highly promising solution in the context of WBAN due to its key features such as wide operational bandwidth, low profile, high data transmission rate at low power, omnidirectional radiation pattern and ease in fabrication. In case of antenna-human body interaction, WBAN is classified in three main types: in-body, on-body, and off-body. An extremely low power is required in proximity of human body to avoid any electromagnetic interaction between antenna and human body. It is well known that the dielectric properties of human tissues changes with frequency, which affect the RF signals characteristics [Quig *et al.*, 2006]. In this study, antenna-human body interaction is carried out mainly in case of on-body and off-body communications. In this scenario, frequency-domain parameters such as antenna efficiency, radiation pattern, gain and input impedance get affected. Whereas, in case of time-domain analysis the received signal waveform shows deterioration [Klemm and Troester, 2006].

Several studies in the context of antenna-human body interactions are reported [Chahat *et al.*, 2011; Koohestani *et al.*, 2013; Tuovinem *et al.*, 2013; Alomainy *et al.*, 2005; See and Chen, 2009]. In [Chahat *et al.*, 2011], a rectangular shaped phantom model, which discards the skin effect, is used for a very small ground UWB antenna. A coplanar-fed UWB monopole antenna in the proximity of human arm is studied in [Koohestani *et al.*, 2013]. The effect of different body tissues such as skin, fat, muscle, and bone thickness in the proximity of on-body communication is carried out in [Tuovinem *et al.*, 2013]. In [Alomainy *et al.*, 2005] and [See and Chen, 2009] a comparative study for different antennas in the context of on-body communication is carried out. In order to achieve the miniaturization in antenna design some techniques are reported in [Bahadori *et al.*, 2007; Abbosh *et al.*, 2009]. However, the dimensions of these antennas are still too large and they cannot be easily integrated with commercial portable systems. Thus, for commercial applications, compactness in antenna design is required in order to have portable systems. Thus, the design of compact UWB antenna, which can work near to human body in

3.1-10.6 GHz band with desired antenna characteristics in frequency-domain and time-domain, is an essential requirement.

The above mentioned issues can be partially resolved by using fractal geometry in the UWB antenna design. Its application helps to achieve the desired compactness as well as wide operational bandwidth due to its self-similar and space filling properties [Werner *et al.*, 1999; Anguera *et al.*, 2005; Hashemi *et al.*, 2006]. The space filling property enhances the effective electrical path length of the antenna in a given smaller area. While, self-similar property helps to generates multiple resonances, which in turn leads to wide operational bandwidth [Werner *et al.*, 1999; Anguera *et al.*, 2005]. Some of the fractal geometries are used in UWB antenna design such as Koch snowflake [Anguera *et al.*, 2005], hexagonal shaped [Werner *et al.*, 1999] and Sierpinski triangle [Werner *et al.*, 1999; Anguera *et al.*, 2005].

UWB technology also faces the multipath fading like other communication technologies due to multiple reflections and refractions in the data transmission path. As we know, multiple-input-multiple-output (MIMO) techniques are popularly used to overcome multipath fading. Thus, in order to resolve above mentioned issues, MIMO technology is combined with UWB technology [Najam *et al.*, 2011; Bolin *et al.*, 2005]. Thus, in this study, fractal UWB antenna and fractal UWB MIMO antenna characteristics are studied in the proximity of human body in order to understand the electromagnetic interaction between antenna and human body.

7.2 Koch Fractal UWB Antenna for On-Body WBAN Applications

7.2.1 Antenna Design

(a) Antenna Configuration

The effect of human body on antenna characteristics is studied using an octagonal shaped Koch fractal UWB antenna with fractal ground. The design and development of this antenna is discussed in section 3.8.1. Koch fractal geometry is used at the edges of octagonal shaped geometry to increase the effective length at outer perimeter in a smaller area. Here, the octagonal geometry works as an initiator, whereas Koch fractal geometry works as a generator in the evolution of antenna design. Moreover, fractal structures with limited number of iterations are generated considering the fabrication and complexity constraints. Thus, the generation of antenna structure using Koch fractal geometry is restrained up to second iteration. With the increment in iterations order series of similar fractal structure with different scaled geometries are repeated continuously, which in turn leads to multiband behavior [Dhar *et al.*, 2013]. It is evident that, the effective area and length of the structure increases with iterations.

To the best knowledge of authors, study for fractal antennas in the closed proximity of human body for on-body communication is not carried out before. The chosen antennas are compact in dimensions as well as shows good antenna characteristics. Figure 7.1 shows the optimized geometry of the antenna. In the design and fabrication of the antenna FR4 substrate of dielectric constant (ε_r) 4.4, loss tangent of 0.025 with thickness of 1.6 mm is used. The ground plane is placed on the other side of the substrate. The presented antenna is simulated and designed using Ansoft HFSS v.13. In the design of antenna, initial substrate dimension is selected as rectangular due to its good wideband and radiation characteristics [Tasouji *et al.*, 2013]. The values of dimension parameters are as: L = 31 mm, L_m = 12 mm, W = 28 mm, W_m = 3 mm, R = 9 mm and L_g = 11mm.

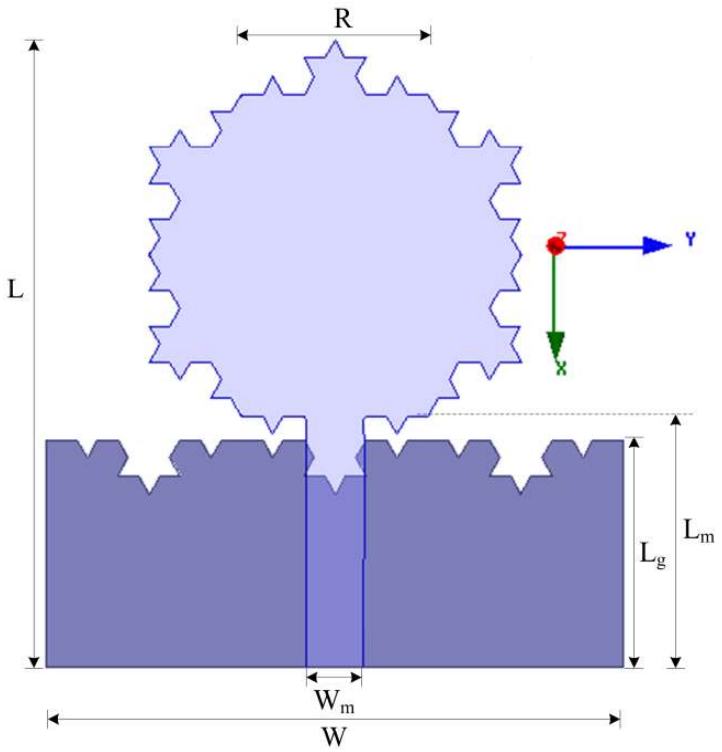

Figure 7.1: Optimized geometry of the presented antenna

(b) Layered Rectangular Human Body tissue model

In this study, the layered rectangular human body tissue model is used to study the variation in antenna behavior in terms of S-parameters as shown in Figure 7.2. The presented model is four layered structure, which contains skin, fat, muscle and bone [Tuovinem *et al.*, 2013] and thickness of each layer is taken as suggested in [Tuovinem *et al.*, 2012]. The electrical properties of human body tissue are shown in Table 7.1 with respective layered thickness; calculated at 7.5 GHz frequency [Dielectric, 2013]. Antenna is placed on the top of the human body model, at the center position.

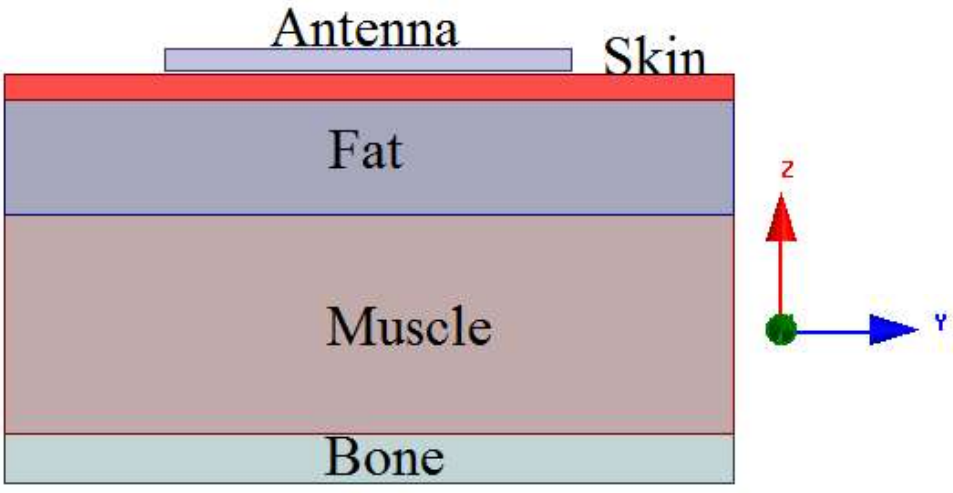

Figure 7.2: Layered Human body tissue model with antenna on its top

Table 7.1: The Electrical Properties of Tissues with Respective Thickness

	Layered Human body tissue model			
Tissue	ε_r	*Tanδ*	*P*	Thickness
Skin	33.6	0.378	1100	1.7 mm
Fat	4.8	0.204	916	8 mm
Muscle	46.2	0.370	1041	10 mm
Bone	8.9	0.417	1990	3.3 mm

(c) Experimental Setup

Figure 7.3 shows the measurement setup established in anechoic chamber to evaluate the S-parameters variation in the context of antenna-body interactions. In the measurement process antenna is placed on the human body (d = 0 mm) and nearby human body (d = 5 mm and d = 10 mm). Here, horn antenna work as a transmitter and fractal UWB antenna work as a receiver. Moreover, the measurements of radiation patterns of the fractal UWB antenna for various body orientations are not practical. Hence, S_{21} is measured, which is related to radiation performance of the antenna and can be easily used to provide a comparative analysis of antenna in free space as well as in proximity of human body. In order to measure the S-parameters, Agilent E5071C vector network analyzer (VNA) is used. In addition, both the antennas are separated approximately 1.5 m from each other to satisfy the far field criteria. In order to provide better performance of antenna-body interaction, the fractal UWB antenna is positioned on the body (d = 0 mm) as well as at a distance of d = 5 mm and 10 mm. The antenna is placed at abdomen, near forehead and on the chest to acquire fetal electrocardiogram (fECG), electroencephalography (EEG) and ECG signals, respectively. Furthermore, horn antenna is rotated from $\theta = 0^0$ to 90^0 in the intervals of 30^0. The orientation $\theta = 0^0$ shows face-to-face alignment, whereas $\theta = 90^0$ corresponds to -*y* axis direction.

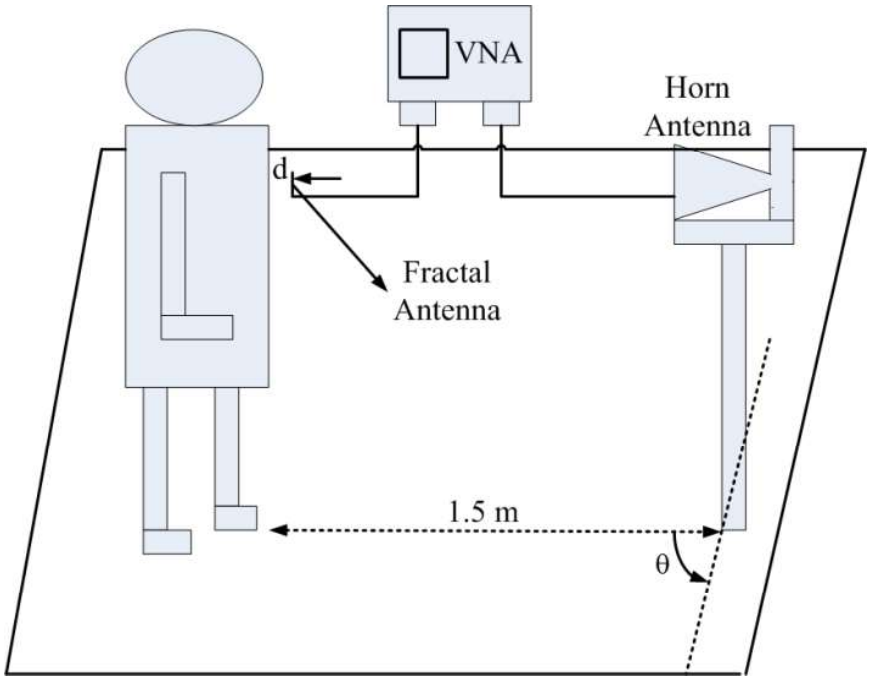

Figure 7.3 Measurement setup in anechoic chamber

7.2.2 Results and Discussions

(a) S-parameters Result

The prototype is fabricated to validate the simulated results. In order to collect the data for healthcare application a measurement setup as shown in Figure 7.3 is designed in the anechoic chamber. The return losses of the antenna in in three different scenarios: Simulation of antenna in free space, Measurement of antenna in free space and antenna behavior on the above discussed tissue model with variation in distance (d) are shown in Figure 7.4. It is observed that S_{11} shows significant variation in the presence of human body. Thus, it can be concluded that, when antenna is close to human body then operating bandwidth of antenna gets altered. However, the presented antenna covers entire operational bandwidth (S_{11}< -10dB) in the UWB range. When antenna is placed on the human body tissue model, it shows an enhancement in operating bandwidth from lower frequency edge of UWB spectrum. It is observed that the antenna shows wideband operational bandwidth in both the cases (free space and on human body tissue model). However, some mismatches are observed because of the fact that accurate estimation of the thickness of the human body tissues is not practically possible.

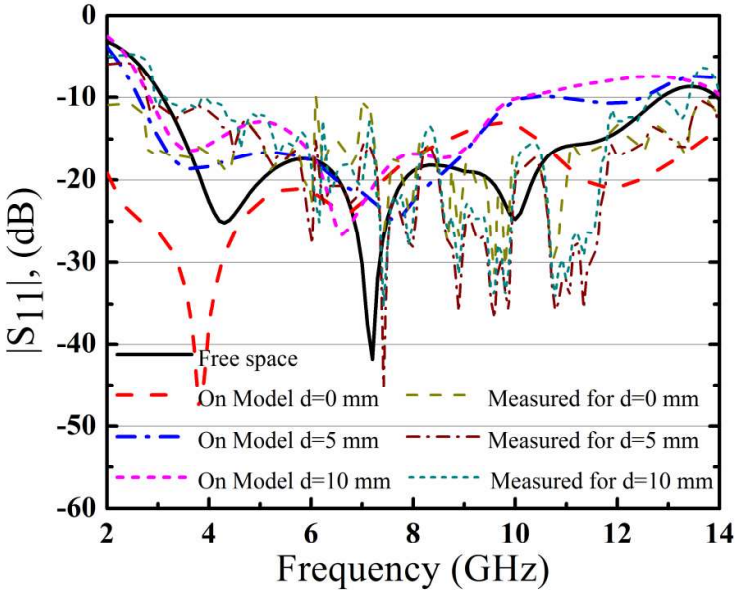

Figure 7.4: Return loss variation of the antenna in free space and in the proximity of human body tissue model

Figure 7.5 displays S_{21} characteristics of the antenna in free space, near forehead, on chest and at abdomen. The distance between presented antenna and the human body in all the above studied cases is varied from d = 0 mm to 15 mm, in the steps of 5 mm. The comparison of S_{21} characteristics of antenna for different orientations (θ = 0°, θ = 30°, θ = 60 ° and θ = 90°) in each of these cases is performed. It is observed from Figure 7.5(a), (b) and (c) that when antenna is at abdomen, for θ = 0°, θ = 30° and θ = 60°, a further attenuation of 5 dB to 15 dB is noticed because of absorption caused by human body. Whereas, for θ = 90° further reduction is observed due to obstruction offered by the human body. This reduces the directional property of the antenna. It can be seen from Figure 7.5(d), (e) and (f), when antenna is placed near to forehead, signals get less attenuated as compared to abdomen scenario. Similar behavior is observed from Figure 7.5(g), (h) and (i), when antenna is placed on chest. It is due to less influence of human body on radiation characteristics of the antenna. It is evident from results that behavior of the antenna get affected utmost in case of on-body communications (d = 0 mm)

compared to off-body communications (d = 5 mm and 10 mm). RF signal characteristics deteriorate when antenna is placed near the human body due to increase in radiation absorption and impedance mismatching. It can be seen from Fig 6(a)-(i) that best response is achieved when presented fractal UWB antenna and horn antenna are in face to face orientation and it gets affected with an increment in angle θ (from 0°-90°) due to the decrease in directional property of the antenna. Figure 7.5(j) shows antenna behavior in free space and it shows very less attenuation due to absence of human body.

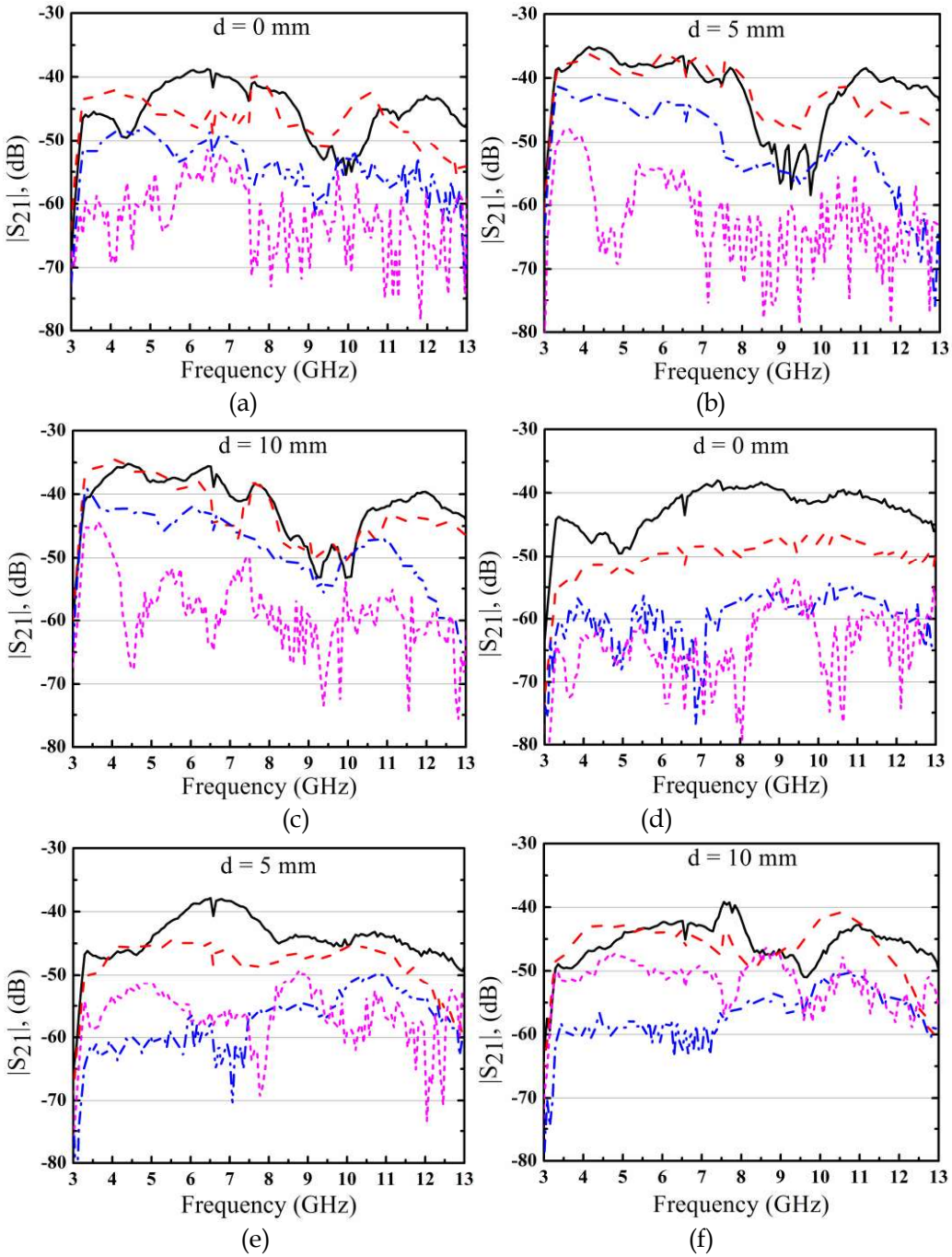

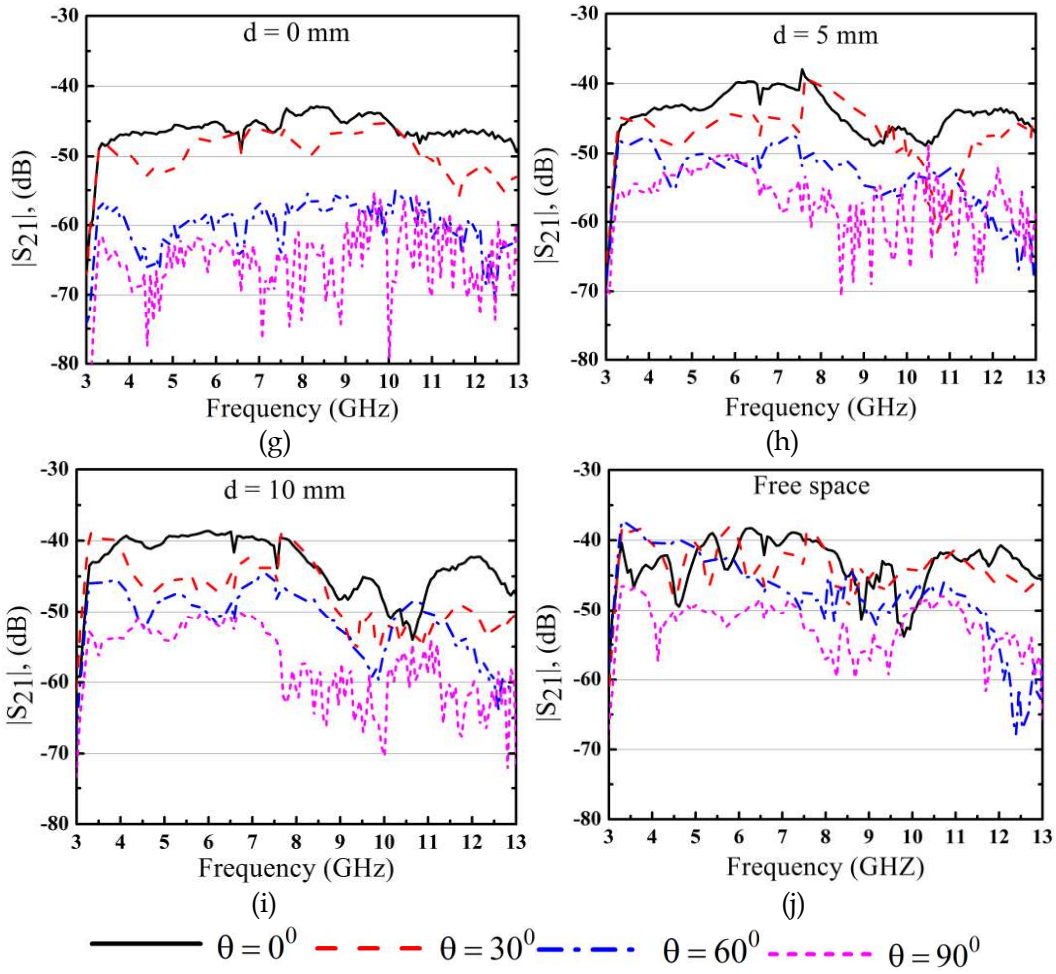

Figure 7.5: Measured S_{21} of the fractal UWB antenna at (a) Abdomen for d = 0 mm, (b) Abdomen for d = 5 mm, (c) Abdomen for d = 10 mm, (d) Near forehead for d = 0 mm, (e) Near forehead for d = 5 mm, (f) Near forehead for d = 10 mm, (g) Chest for d = 0 mm, (h) Chest for d = 5 mm, (i) Chest for d = 10 mm and (j) Free space

(b) Radiation Performance

Figure 7.6 shows the comparative study of radiation patterns at 4.3, 7.2 and 10 GHz resonant frequencies in three different scenarios: Simulation of antenna in free space, Measurement of antenna in free space and antenna behavior on the above discussed tissue model for d = 0 mm. It can be seen that radiation pattern is nearly omnidirectional in free space, whereas it shrunk significantly in the proximity of human body.

(c) Group Delay

The study of phase linearity of antenna is essential in case of UWB antenna and demonstrated in terms of group delay performance. It is evident From Figure 7.7 that the presented antenna shows nearly flat group delay response in the entire UWB band with and without tissue model. However, small group delay variation is observed in the 6-8 GHz frequency band, without tissue model and with tissue model for d = 5 and 10 mm. In addition, when the antenna is in contact with the tissue model then small group delay variation is observed in 3.9 GHz frequencies because of absorption by human tissue model.

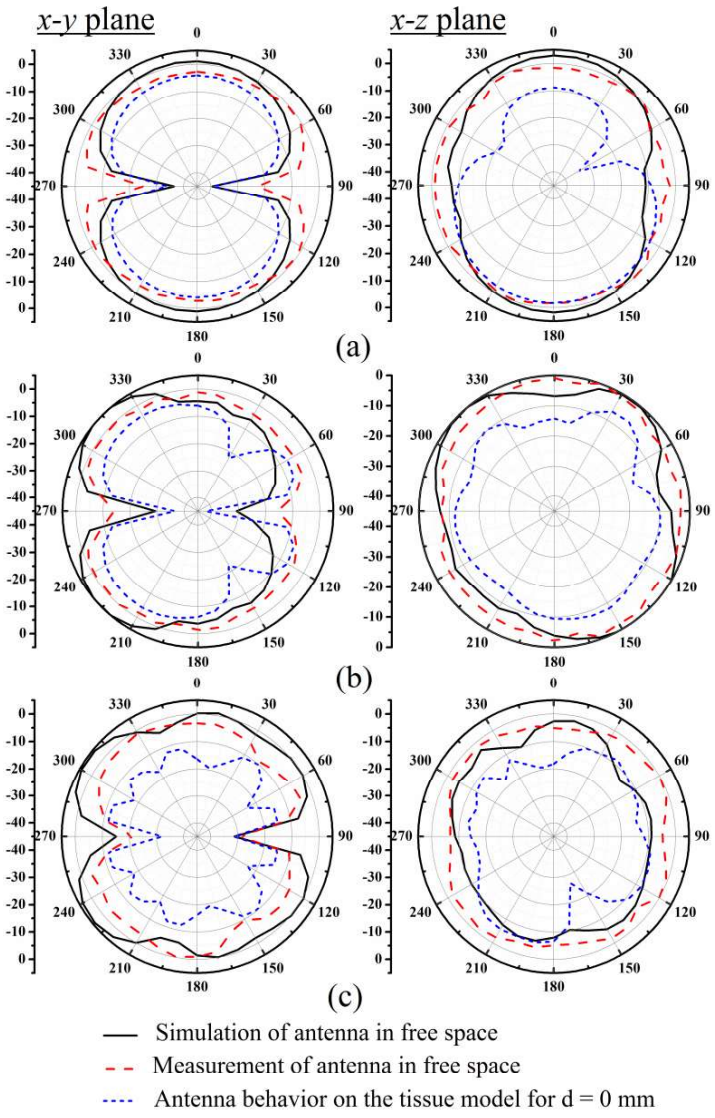

Figure 7.6: Measured and simulated radiation pattern in the xy-plane and xz-plane at 4.3, 7.2 and 10 GHz resonant frequencies (a) 4.3 GHz, (b) 7.2 GHz and (c) 10 GHz

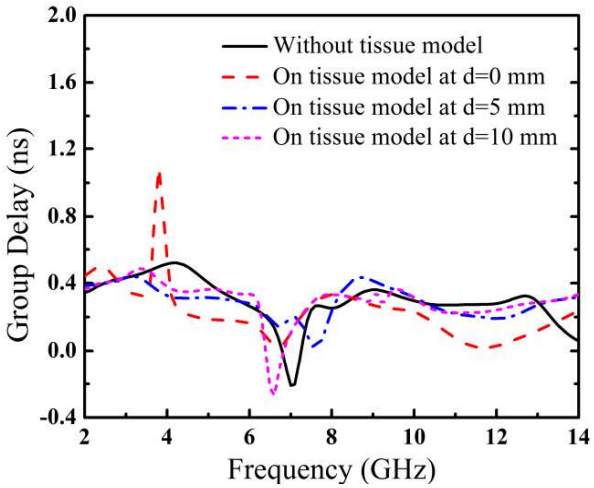

Figure 7.7: Group delay of the fractal antenna with and without human body tissue model

(d) Specific Absorption rate (SAR)

The investigation of exposure of RF to human body in terms of SAR is essential for on-body and off-body WBAN communications. It is due to the absorption of electromagnetic power by the surrounding body tissue. Thus, the SAR (W/kg) is calculated as the power absorbed by the tissue per unit of mass, using a SAR line which passes through maximum SAR, and expressed as [Sanchez, 2009]:

$$SAR = \frac{\sigma}{\rho}|E|^2 \tag{7.1}$$

where σ (S/m) represents tissue conductivity, ρ (kg/m^3) shows tissue density and E is root mean square value of electric field. Here, in the calculation, we used 1gm averaging mass standard, the IEEE C95.3 averaging method and reference power of 1W (rms). The SAR variation with distance is shown in Figure 7.8. It is seen that the obtained SAR values are too high compared to SAR standard limit 1.6 W/kg over 1gm of tissue. By scaling the power value up to 3.69 mW, desired SAR level can be obtained.

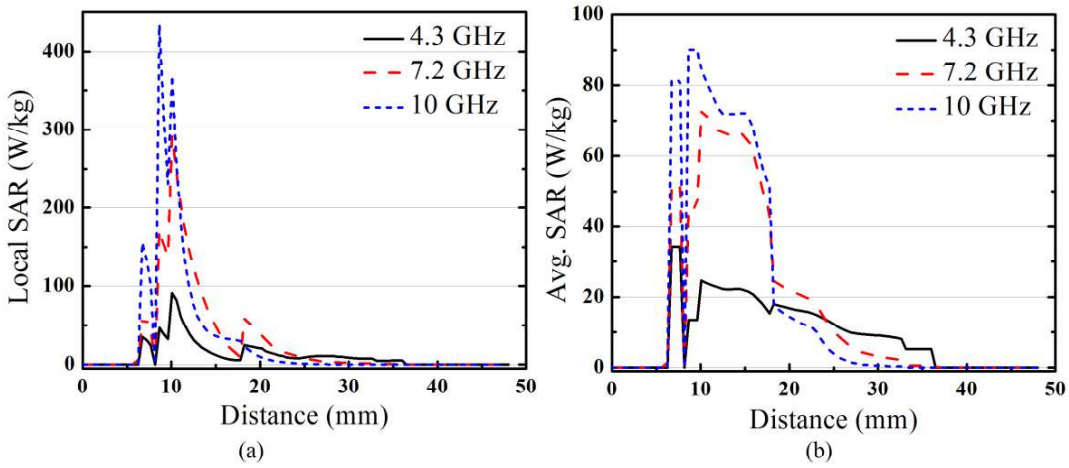

Figure 7.8: SAR variation with distance (a) Local SAR and (b) Avg. SAR

7.3 Koch Fractal UWB MIMO Antenna for On-Body WBAN Applications

7.3.1 Antenna Design

(a) Antenna Configuration

In this section, the effect of human body on antenna characteristics is studied using an octagonal shaped fractal UWB MIMO antenna. Figure 7.9 shows the optimized geometry of the proposed antenna. The design and development of this antenna is explained in section 3.4.1. In the design and fabrication of the antenna FR4 substrate of dielectric constant (ε_r) 4.4, loss tangent of 0.025 with 1.6 mm thickness is used. The ground plane is positioned on the other side of the substrate. The proposed antenna is simulated and designed using Ansoft HFSS v.13. The application of Koch fractal geometry at the edges of octagonal shaped geometry helps to achieve miniaturization and wideband characteristics. The band rejection is achieved in WLAN band by etching a C-shaped slot from each fractal monopole (FM). In addition, transmission response (S_{21}) is studied with the variation in distance between selected antennas to analyze the radiation behavior at different human body positions to acquire the healthcare signals (near to

forehead, chest and abdomen). In addition, an experimental set up, which contains horn antennas as the transmitting antenna and UWB MIMO antenna near to human body as receiving antenna are placed in the anechoic chamber as mentioned in section 7.2.1 (c). In order to provide more insight into behavior of the antenna in proximity of human body layered human body tissue model is used as mentioned in section 7.2.1 (b). To the best knowledge of authors, study for fractal UWB MIMO antennas in the proximity of human body for on-body/near-body WBAN communication is not carried out previously. The optimized values of design parameters are as: L = 25 mm, W = 40 mm, R = 4.6 mm, W_m = 2.6 mm, L_g = 8.5 mm, T = 0.3 mm, d = 0.8 mm, L_1 = 1.2 mm, L_2 = 3.4 mm, L_3 = 7 mm, L_4 = 2.6 mm, L_5 = 15.5 mm, L_6 = 1 mm, L_7 = 6.25 mm, W_1 = 6.2 mm, W_2 = 9.2 mm, L_{s1} = 3.5 mm, W_{s1} = 1 mm, L_{s2} = 1.5 mm, W_{s2} = 5 mm, L_{s3} = 1 mm, W_{s3} = 1.5 mm, L_{s4} = 2 mm, W_{s4} = 8 mm, L_{s5} = 1 mm, and W_{s5} = 2 mm.

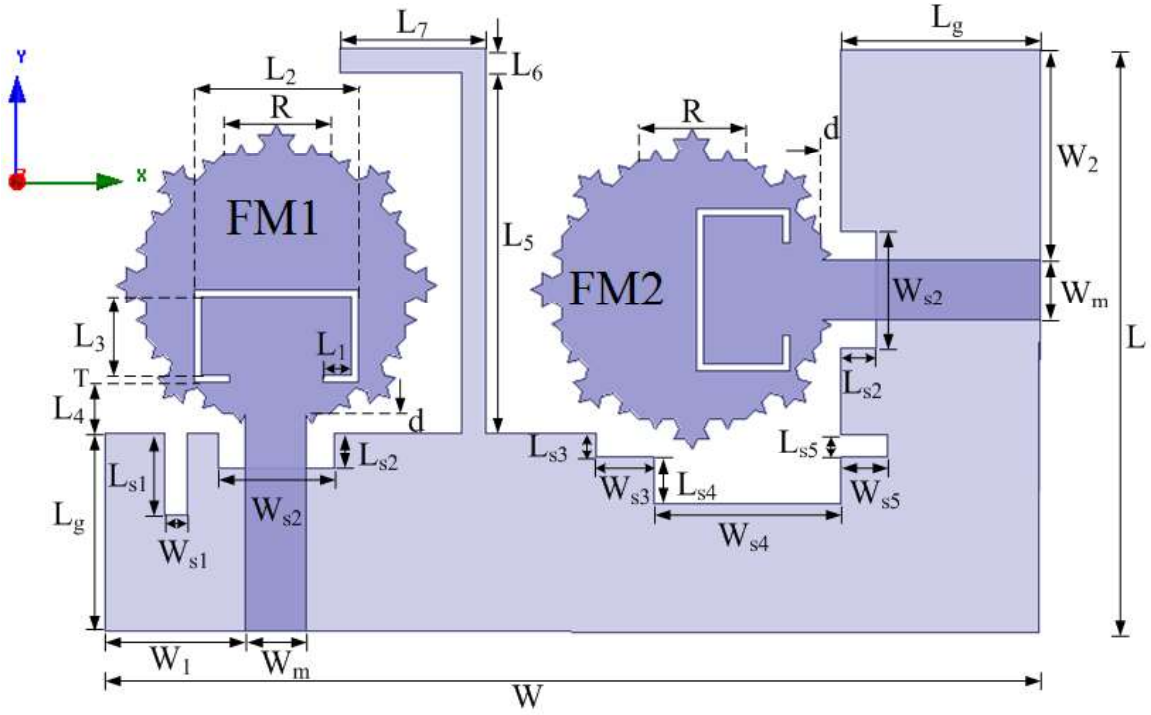

Figure 7.9: Optimized geometry of the presented antenna

7.3.2 Results and Discussions

(a) S-parameters Result

The proposed antenna prototype is fabricated to validate the simulated results. The return loss (S_{11}) performances of the antenna in three scenarios are shown in Figure 7.10: Simulated S_{11} (free space), Measured S_{11} (free space) and Simulated S_{11} (on layered human body tissue model). In the measurement process, port 1 is excited and 50Ω load is used for matching at port 2. In addition, antenna is positioned at the top at its center position of the layered human body tissue model. It is observed that the operational bandwidth of antenna enhanced at lower frequency edge and as at higher frequency edge with small acceptable deterioration in middle UWB band, which in turn helps to cover operational bandwidth more than 2-14 GHz in the proximity of layered human body tissue model. However, band rejection performance in WLAN band is deteriorated because of reflections from tissue. These reflections cause degradation in the amplitude of signal as well as minor shifting in operational bandwidth.

However, a good agreement is perceived between measured S_{11} results and simulated results, except WLAN spectrum.

The measured S_{21} characteristics of the fabricated antenna are provided in four scenarios: free space, near forehead, on chest and at abdomen, as shown in Figure 7.11. In addition, the space between antenna-human body changed from d = 0 mm to 15 mm, in the step size of 5 mm and antenna behavior for on-body and near to body scenarios is evaluated. Moreover, an assessment of S_{21} behavior of the antenna for variation in human body orientations w.r.t. horn antenna as shown in experimental setup for θ = 0° to θ = 90° in the step size of θ = 30° is carried out for above specified body locations. Antenna performance near to abdomen for θ = 0°, θ = 30° and θ = 60° is shown in Figure 7.11(a), (b) and (c). Attenuation between 5-15 dB is noticed because of absorption of RF signals by the human body, this leads to mismatch in impedance performance. However, in case of $\theta = 90^0$ the directional behavior of the antenna decreases because of blockage offered by human body, which leads to further attenuation. The performance of the antenna near to forehead is displayed in Figure 7.11(d), (e) and (f). It is noticed that the antenna shows less attenuation compare to different orientation of abdomen cases, because forehead of the human body contains less amount of fat layer thickness compared to abdomen. In these circumstances, radiation characteristics of the antenna get less attenuated. Moreover, from Figure 7.11(g), (h) and (i) similar behavior is noticed when the antenna is positioned near to the chest. Thus, from S_{21} behavior of the antenna shown in Figure 7.11(a)-(i) it is noticed that antenna characteristics gets affected most in case of on-body (d = 0 mm) scenario compared to nearby cases (d = 5 mm and 10 mm) due to deterioration in RF signal characteristics in the proximity of the human body. These deteriorations in S_{21} are noticed because of enhancement in radiation absorption, which leads to impedance mismatching. Moreover, face to face orientation of the proposed antenna and horn antenna provide best response and it degraded further with the increment in orientation angle θ (from 0°-90°) because of decrease in directional property of the antenna. Figure 7.11(j) shows the S_{21} characteristics of the antenna in free space. It can be seen that very less attenuation is noticed due to absence of human body. In addition, around WLAN notch band sharp band attenuation is observed in all the above discussed cases.

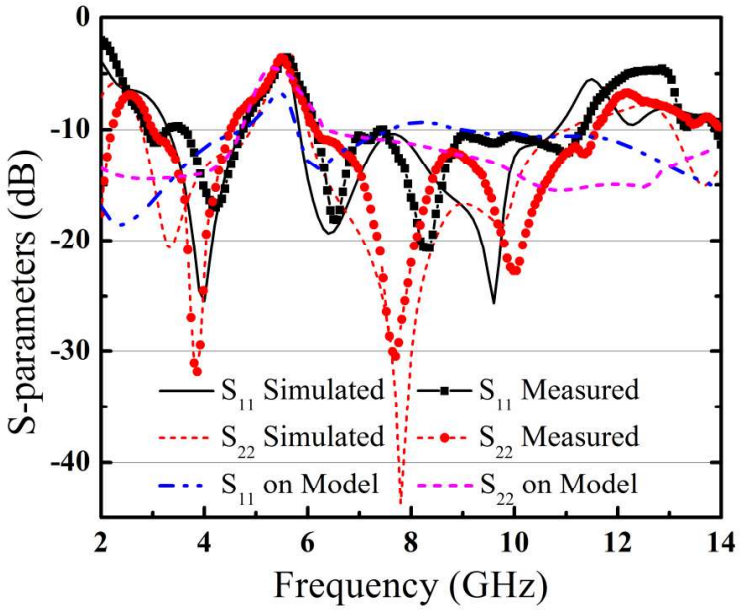

Figure 7.10: Return loss variation of the antenna in free space and in the proximity of human body tissue model

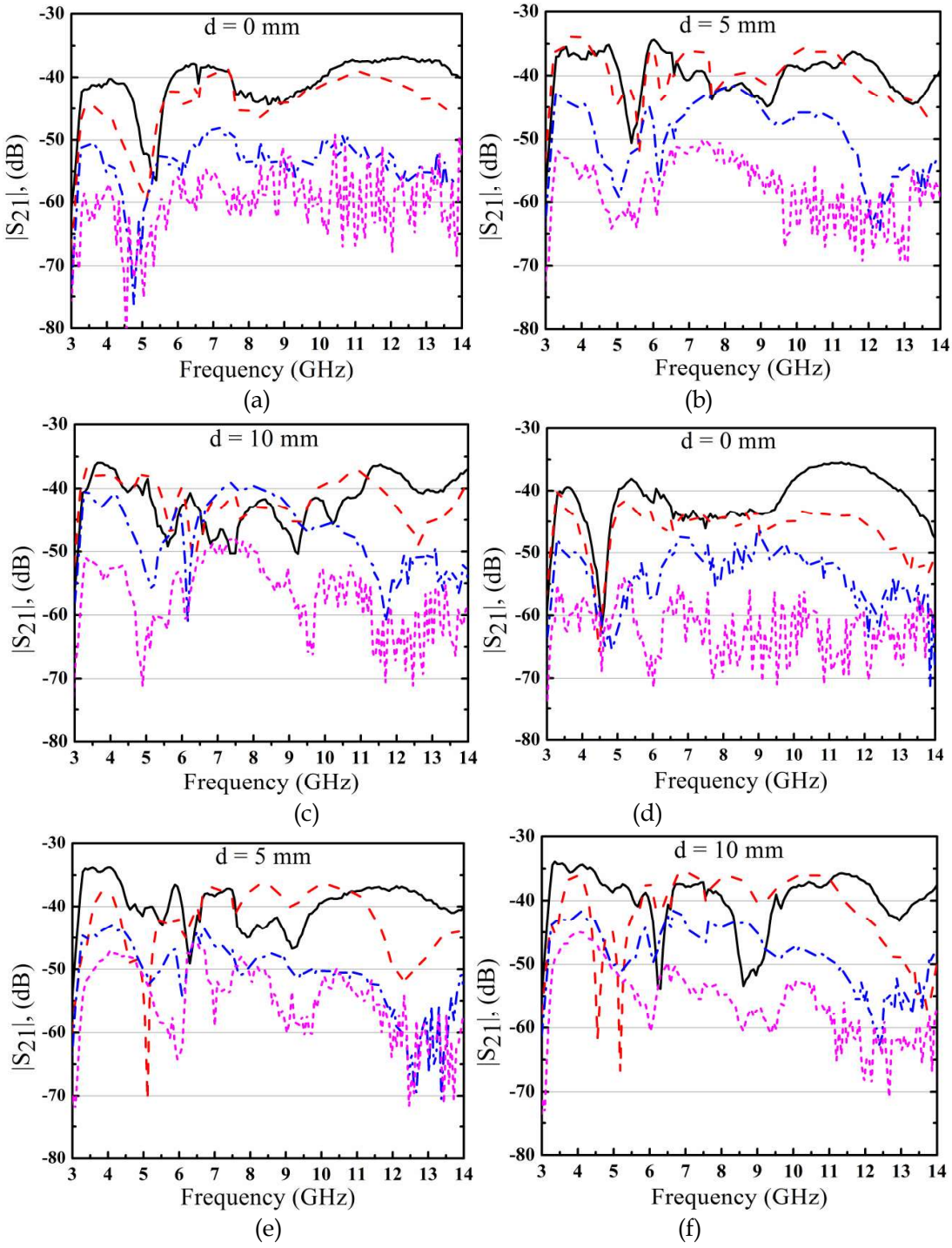
d = 0 mm
d = 5 mm
d = 10 mm
d = 0 mm
d = 5 mm
d = 10 mm
|S21|, (dB)
Frequency (GHz)
(a)
(b)
(c)
(d)
(e)
(f)

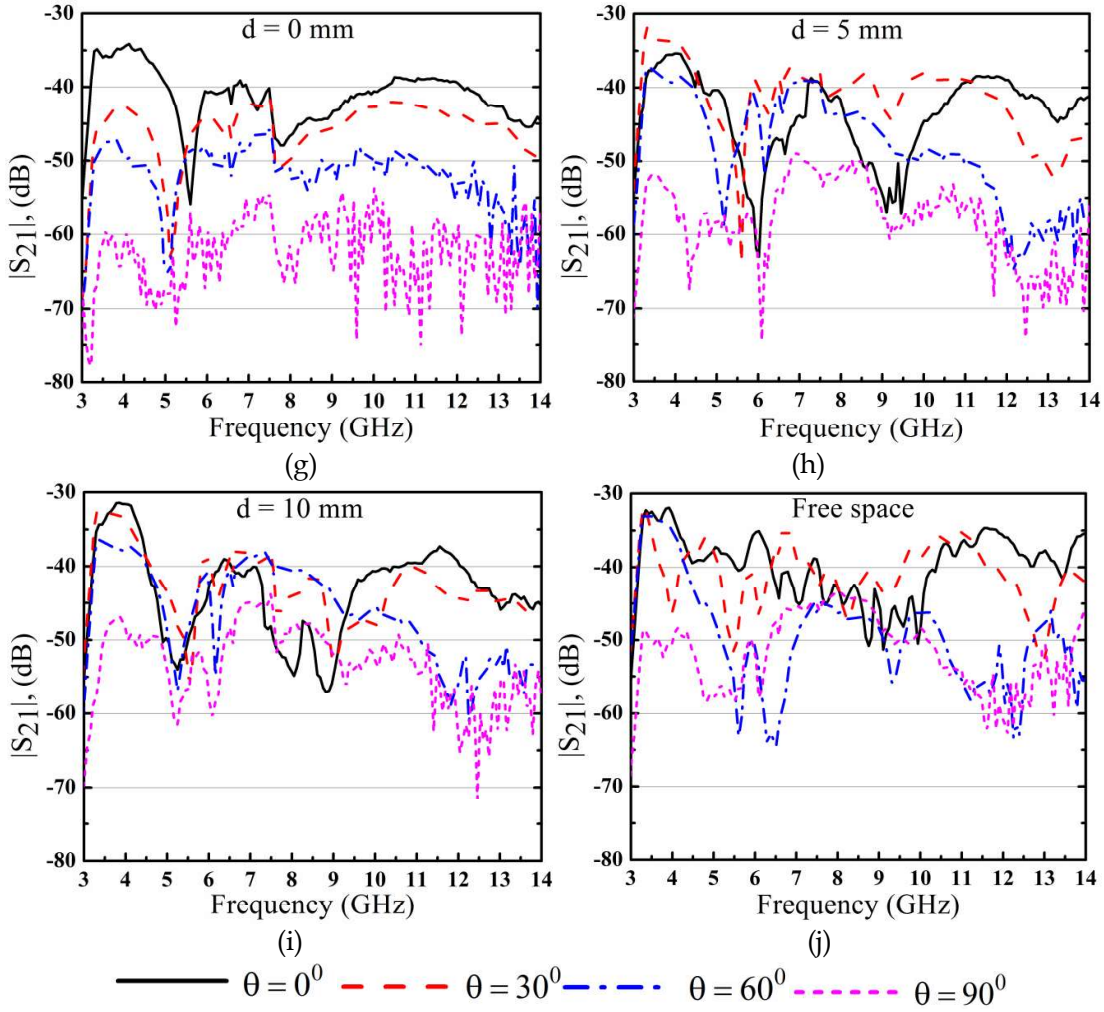

Figure 7.11: Measured S_{21} of the fractal UWB antenna at (a) Abdomen for d = 0 mm, (b) Abdomen for d = 5 mm, (c) Abdomen for d = 10 mm, (d) Near forehead for d = 0 mm, (e) Near forehead for d = 5 mm, (f) Near forehead for d = 10 mm, (g) Chest for d = 0 mm, (h) Chest for d = 5 mm, (i) Chest for d = 10 mm and (j) Free space

(b) Radiation Performance

Figure 7.12 and 7.13 shows the investigations of on-body radiation performance of the presented fractal UWB MIMO antenna at 4.3, 7.2 and 10 GHz resonant frequencies in three different scenarios: Simulated S_{11} (free space), Measured S_{11} (free space) and Simulated S_{11} (on layered human body tissue model at d = 0 mm), for port 1 and port 2, respectively. During the measurements, port 1 is excited and port 2 is matched with 50Ω load, and vice versa. It is observed that radiation pattern is nearly omnidirectional in free space, whereas it shrunk considerably in the proximity of human body tissue model compared to free space simulated and measured results of the antenna. It is due to reflections caused by layered human body tissue model. It is noticed that at higher resonant frequency, radiation pattern gets deteriorated compare to lower resonant frequency because of the change in current nature. Moreover, multiple bends and curves in fractal geometry causes the variation in current path, which in turn leads to enhanced radiation characteristics of the antenna and helps to obtain the stable radiation pattern [Fereidoony *et al.*, 2012].

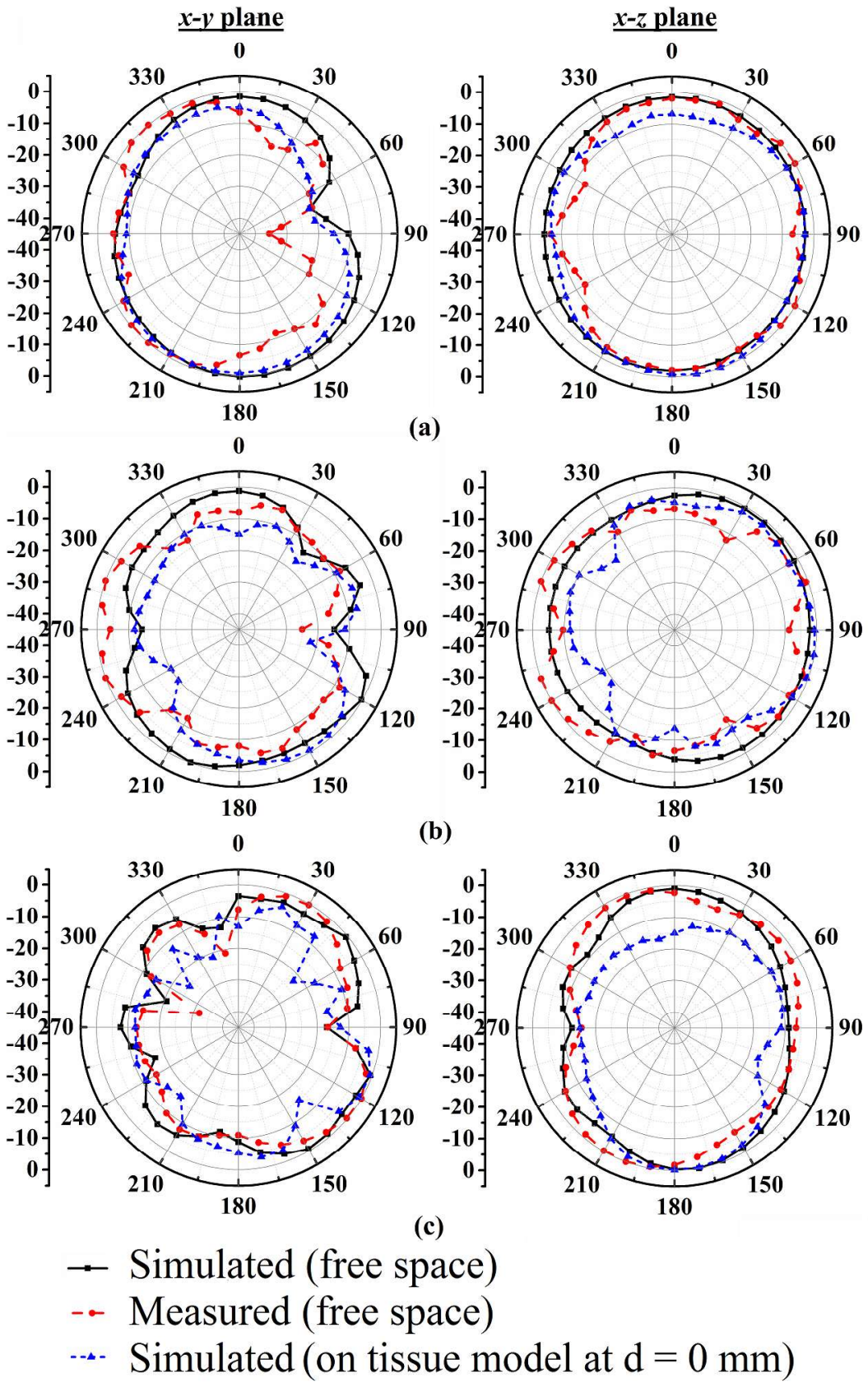

Figure 7.12: Measured and simulated radiation pattern in the xy-plane and xz-plane, when port 1 is excited and port 2 is matched with 50Ω load, at resonant frequencies (a) 4 GHz, (b) 6.5 GHz and (c) 9.6 GHz

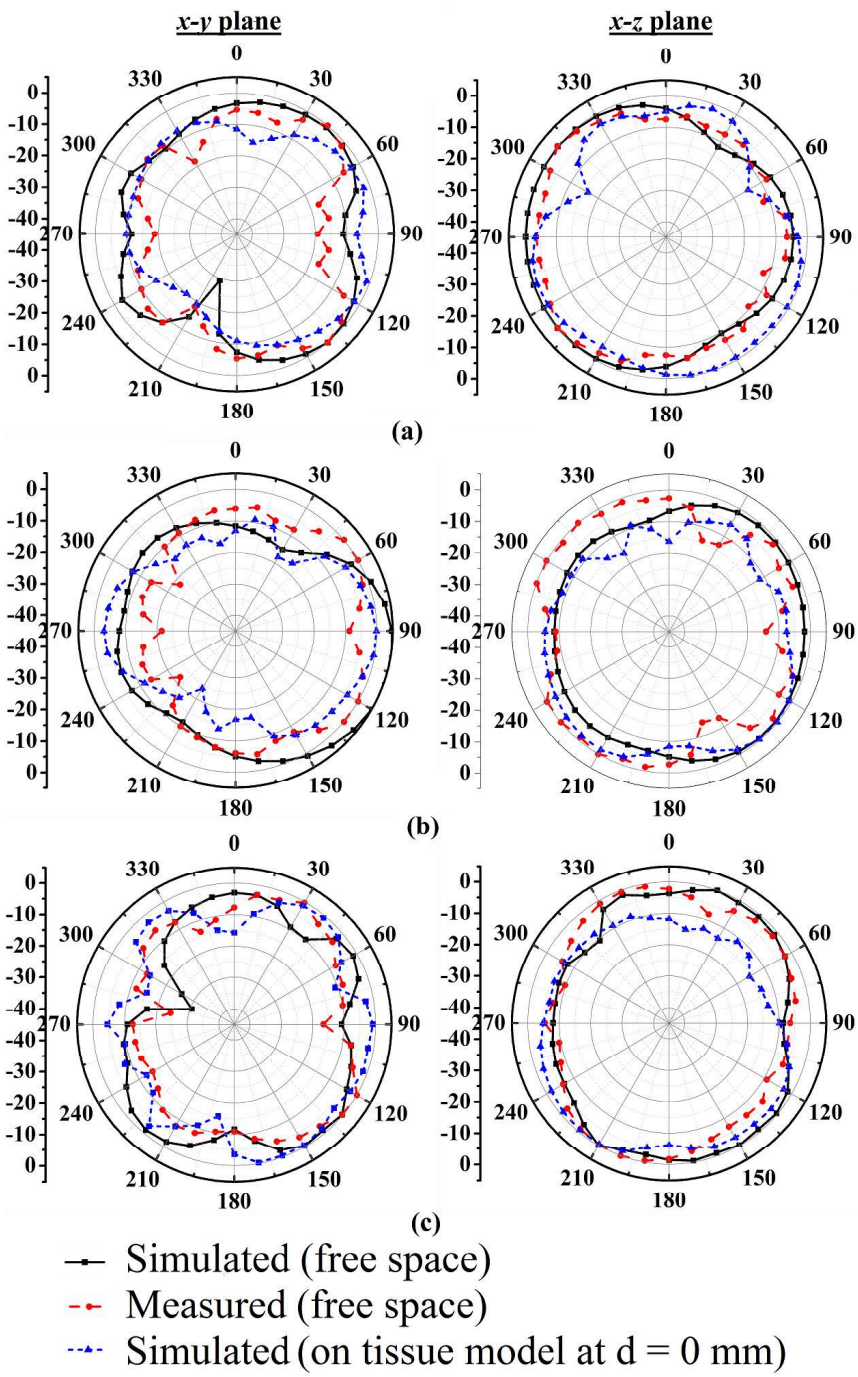

Figure 7.13: Measured and simulated radiation pattern in the xy-plane and xz-plane, when port 2 is excited and port 1 is matched with 50Ω load, at resonant frequencies (a) 4 GHz, (b) 6.5 GHz and (c) 9.6 GHz

(c) Group Delay

The evaluation of phase linearity of antenna is crucial in case of UWB antenna and evaluated in terms of group delay. It can be seen from Figure 7.14 that, the presented antenna shows flat group delay response in the UWB band with and without tissue model. However, small group delay is observed in the 6-8 GHz frequency band, without tissue model and with tissue model for d = 5 and 10 mm away from tissue model. In addition, when the antenna is in direct contact with the tissue model then small group delay is observed in 3.9 GHz frequencies because of absorption by human tissue model.

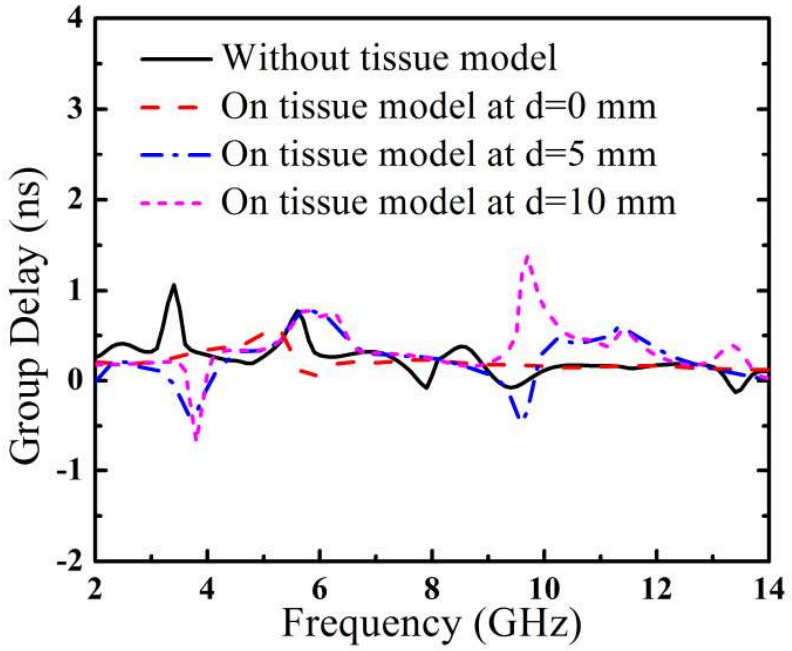

Figure 7.14: Group delay of the fractal antenna with and without human body tissue model

(d) Specific Absorption rate (SAR)

The examination of exposure of RF signal in the proximity of human body in terms of SAR is essential for WBAN communications because electromagnetic power is absorbed by the surrounding body tissue. The SAR variation of the antenna with variation in distance is displayed in Figure 7.15 for port-1 and port-2. When port-1 is excited, then port-2 is matched with 50Ω load, and vice versa. It is seen that the obtained SAR values are too high compared to SAR standard limit 1.6 W/kg over 1gm of tissue. The power and SAR value has a linear mathematical relation, so it can be easily scaled. Thus, to obtain the SAR level below SAR standard, power level should be kept less than 2.67 mW.

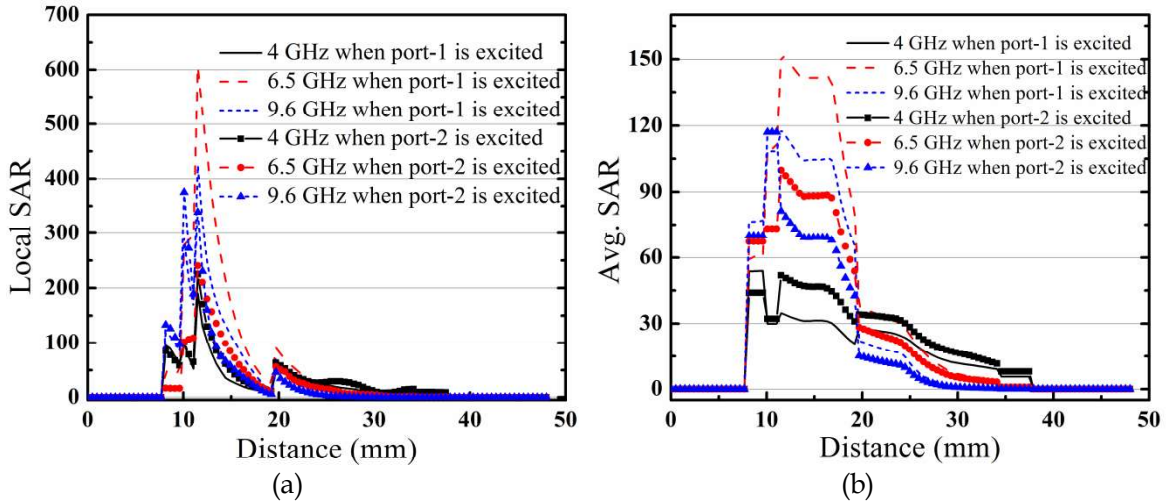

Figure 7.15: SAR variation with distance (a) Local SAR and (b) Avg. SAR

Table 7.2: Comparison of the proposed work with others work presented in the literature

Antenna	Dimensions (mm×mm×mm)	Bandwidth (GHz) Free space/On-body
Work in Section 6.3	31×28×1.6	3-12.8/2.8-13.6
Work in Section 6.4	25×40×1.6	3.3-10.8/2.9-10.6
Chahat *et al.*, 2011	25×10×1.6	3.1-10.6/3.1-11.2
Koohestani *et al.*, 2013	44×38×1.57	2.5-4.5, 7-8.6
See and Chen, 2009	35×25×0.8	2.6-5.6/2-6
Tuovinem *et al.*, 2013	30×40×1.57	3-14/1.5-13

7.4 Summary

This chapter investigated two types of fractal antennas behavior in the context of on/off-body BAN communications. In this study, to analyze the effect of human body tissues on antenna performance, a four layered human body tissue model is used. The effects of human body on antenna characteristics are investigated in terms of S_{11} and S_{21} parameters. Moreover, S_{21} characteristics of the antenna for different orientations at different body parts such as abdomen, near forehead and chest are performed to acquire the healthcare signals. In the first section, fractal UWB antennas characteristic are analyzed experimentally for on-body and off-body BAN scenarios. S_{11} performance in free space (simulated and measured) and on layered human body tissue model shows that the presented antenna has wideband operational bandwidth in each case. It is evident from results that the antenna has a good radiation behavior in the proximity of the human body. Local SAR and avg. SAR values vary with frequency as well as with separation between antenna and human body. In the second section, fractal UWB MIMO antenna characteristics are investigated experimentally in on/off-body WBAN scenarios and shows desired antenna characteristics. Table 7.2 present, a comparative study between presented work in the chapter (fractal UWB antenna and Fractal UWB MIMO antenna) and similar work proposed in the literature in the context of on/off-body WBAN scenarios. Comparative study is provided in terms of dimension and S_{11} characteristics (in free space and on/off-body WBAN). Thus, it can be concluded from results that both the antennas are appropriate choice to work either in free space or in on/off-body WBAN scenarios due to its efficient design.

…